

*Original Research*

# Exploring the Lifelong Changes of Interaction between Cingulo-Opercular Network and Other Cognitive Control Related Functional Networks Based on Multiple Connectivity Indices

Bukui Han<sup>1,2,†</sup>, Guodong Wei<sup>1,2,†</sup>, Fengyu Dou<sup>1,2</sup>, Junhui Zhang<sup>1,2</sup>, Xiaotong Wen<sup>1,2,3,\*</sup><sup>1</sup>Department of Psychology, Renmin University of China, 100872 Beijing, China<sup>2</sup>Laboratory of the Department of Psychology, Renmin University of China, 100872 Beijing, China<sup>3</sup>Interdisciplinary Platform of Philosophy and Cognitive Science, Renmin University of China, 100872 Beijing, China\*Correspondence: [wenxiaotong@163.com](mailto:wenxiaotong@163.com) (Xiaotong Wen)

†These authors contributed equally.

Academic Editor: Gernot Riedel

Submitted: 6 October 2022 Revised: 19 January 2023 Accepted: 31 January 2023 Published: 16 May 2023

## Abstract

**Background:** The cingulo-opercular network (CON) has been proposed to play a central role in cognitive control. The lifetime change mechanism of its integrity and interaction with other cognitive control-related functional networks (CCRN) is closely associated with developing cognitive control behaviors but needs further elucidation. **Methods:** The resting-state functional magnetic resonance imaging data were recorded from 207 subjects, who were divided into three age groups: age 4–20, 21–59, and 60–85 years old. For each group, multiple indices (cross-correlation, total interdependence, and Granger causality) within CON and between CON and other cognitive control-related functional networks (dorsal attention network, DAN; central executive network, CEN; default mode network, DMN) were calculated and correlated with age to yield maps that delineated the changing pattern of CON-related interaction. **Results:** We found three main results. (1) The connectivity indices within the CON and between CON and the other three CCRNs showed significant enhancement from childhood to early adulthood (age 4–20 years), (2) mild attenuation within CON from early adulthood to middle age (age 21–59 years), and (3) significant attenuation within CON and between CON and DMN in the elder group (age 60–85 years). **Conclusions:** The results indicated the prominently increased integrity of within-CON and CON-CCRN communication, mildly weakened within-CON communication, and significantly attenuated within-CON and CON-DMN communication, characterizing distinct changing patterns of CON-interaction at three different stages that covered a life-long span.

**Keywords:** cingulo-opercular network; cognitive control related network; functional connectivity; total interdependence; granger causality; life-long change

## 1. Introduction

Accumulating evidence has suggested that the dorsal anterior cingulate cortex (dACC) and bilateral anterior insula/operculum (AI) may form a cingulo-opercular network (CON) that is important for cognitive control [1–4]. A growing number of studies have shown that the CON is also extensively involved in attention, decision-making, monitoring, solving conflict, and various tasks that demand cognitive control [5–8]. For example, CON showed sustained activation across cognitively demanding tasks [9].

Chai *et al.* [10] found that the causal influence among CON was associated with the demands of control during a task. On the one hand, some researchers suggested that CON is a monitor which collects important information from other systems to facilitate control. Accordingly, Seeley *et al.* [4] named the network a “salient network” to emphasize its role in integrating emotional and internal sensory information and making behavioral responses to subjective salience. On the other hand, more and more studies proposed that the network may also play a central role of control in goal-directed behavior by exerting control sig-

nals to regulate other systems [11–13]. Those systems include several well-proposed functional networks closely related to cognitive control. For example, the dorsal attention network (DAN) and central executive network (CEN) were also found activated in many demanding tasks and were proposed to be important for attention control and executive functions [14–16], while the default mode network (DMN) which showed deactivation during demanding tasks and was proposed to be a source of internal interference to the cognitive control [17]. Sridharan *et al.* [13] proposed a triple modulation model of the CON, in which the CON initiates cognitive control signals hierarchically by switching activation/deactivation of the Frontal-parietal network (FPN) and DMN. In line with this modulatory model, Chen *et al.* [18] found that transcranial magnetic stimulation (TMS) to the CON and the DAN/CEN nodes influences their functional connectivity with DMN. Furthermore, aberrant interactions of the CON with other functional networks are thought to underlie the physiology of many psychiatric and neurological-related disorders such as depression [19], Insomnia [20], and autism [21]. The studies mentioned



above highlighted the importance of the interaction between CON and other systems in daily life.

Furthermore, researchers also demonstrated that change in the interaction between CON and the other cognitive control related systems might be a prominent characteristic of the development of the brain and closely related to the development of one's behavior. Many studies on children, adolescents, and young adults have shown increased connectivity between CON and other networks when age is increased. The evidence comes from both functional connectivity (FC) analysis [22–24] and structural connectivity analysis [23,25]. More recently, the structural covariance also showed that the modular density of the DMN and FPN systems showed an increasing trend with age [26]. The studies mentioned above suggested maturing pattern of the communication of the CON and other networks. However, many of the previous studies primarily focused on children and adolescents. In contrast, studies on how CON interaction changes in middle-aged and older adults are inadequate. Methodically speaking, many previous studies relied on single connectivity indices such as cross-correlation-based FC analysis and structural connectivity-based analysis, which could not assess the directional information of the interaction between CON and the other networks. Therefore, how the interactions between CON and other cognitive control-related networks change at different ages in lifespan requires further comprehensive investigation, which may provide an important clue to understanding the development of cognitive control in humans.

To assess the question, the present study adopted multiple connectivity approaches, including classical cross-correlation-based FC analysis, total interdependence (TI) analysis, and Granger causality (GC) analysis, to comprehensively elucidate the changing pattern of the interaction between CON and other cognitive control-related networks, including DAN, CEN, and DMN, at different age stages across the lifespan. The TI and the GC analysis take the temporal mutual information into account, and the latter can provide direction and strength of the information flow between brain regions/networks. The study may help to provide a comprehensive connectivity change model related to CON.

## 2. Materials and Methods

### 2.1 Data Source and Participants

The dataset was acquired from the NKI/Rockland Sample database ([http://fcon\\_1000.projects.nitrc.org/indi/pro/nki.html](http://fcon_1000.projects.nitrc.org/indi/pro/nki.html)), including the imaging data recorded from 207 participants aged 4–85 years old. All participants underwent semi-structured diagnostic psychiatric interviews and completed a battery of psychiatric, cognitive, and behavioral assessments. All participants had no history of taking medicine, psychiatric illness, or any brain surgery that might affect their central neural system; they had no serious unstable illnesses requiring medication or hospital-

ization, including hepatic, renal, gastroenterology, respiratory, cardiovascular (including ischemic heart disease), endocrinologic, neurologic, immunologic, or hematologic disease; were not pregnant, breastfeeding, or had other contraindications to magnetic resonance imaging (MRI) at the time of the study. All participants signed a written informed consent form according to the Helsinki Declaration and satisfied the criteria for MRI. The Ethics Committee of the Department of Psychology at Renmin University of China authorized the current analysis procedure.

### 2.2 MRI Data Acquisition

All participants were scanned using a 3-Tesla magnetic resonance scanner (B15, Siemens AG, Munich, Germany). They were required to remain quiet, relaxed, and awake during the ten-minute resting state scanning session with their eyes closed and heads fixed using comfortable sponge fixators. Functional images were acquired using a single-shot T2-weighted gradient-echo-planar imaging (EPI) sequence. The scanning parameters were as follows: repetition time = 2500 ms, echo time = 30 ms, flip angle = 90°, matrix size = 64 × 64, field of view (FOV) = 216 mm × 216 mm, slice number = 38 (axial interleaved acquisition), slice thickness = 3.0 mm, voxel size = 3.0 mm × 3.0 mm × 3.0 mm.

### 2.3 Data Preprocessing

Raw fMRI data were preprocessed using the DPABI toolbox [27] in MATLAB 2013a. The first ten volumes were removed to remove potentially unstable signals. The image preprocessing procedures include slice-timing, realignment to correct head motion, spatial normalizing of the individuals' images to a standardized spatial Montreal Neurological Institute (MNI) space [28], resampling to the voxel size of 3.0 mm × 3.0 mm × 3.0 mm, and spatial smoothing using an 8 mm full-width at half maximum Gaussian kernel to reduce spatial noise [29]. Several optimized denoising procedures were used to reduce spurious temporal signals further. We (1) implemented independent components analysis to remove nuisance components [30] using the GIFT v4.0 toolbox (<http://mialab.mrn.org/software/gift>); (2) scrubbing procedure to detect and correct the time points with a frame-wise-displacement larger than 0.5 mm [31] and replace them with temporal interpolation; (3) regressing out the global noise, white matter signal, cerebrospinal fluid signal, and the head motion parameters as nuisances; we performed global signal removal because the common noise embedded in the global signal may cause severe contamination by false-positive correlation in traditional FC analysis and severely degrade the estimation of TI and GC; (4) detrending to remove signal drift; and (5) bandpass (0.01–0.08 Hz) filtering to acquire a stable low-fluctuating blood oxygenation level dependent (BOLD) signal [10,32].

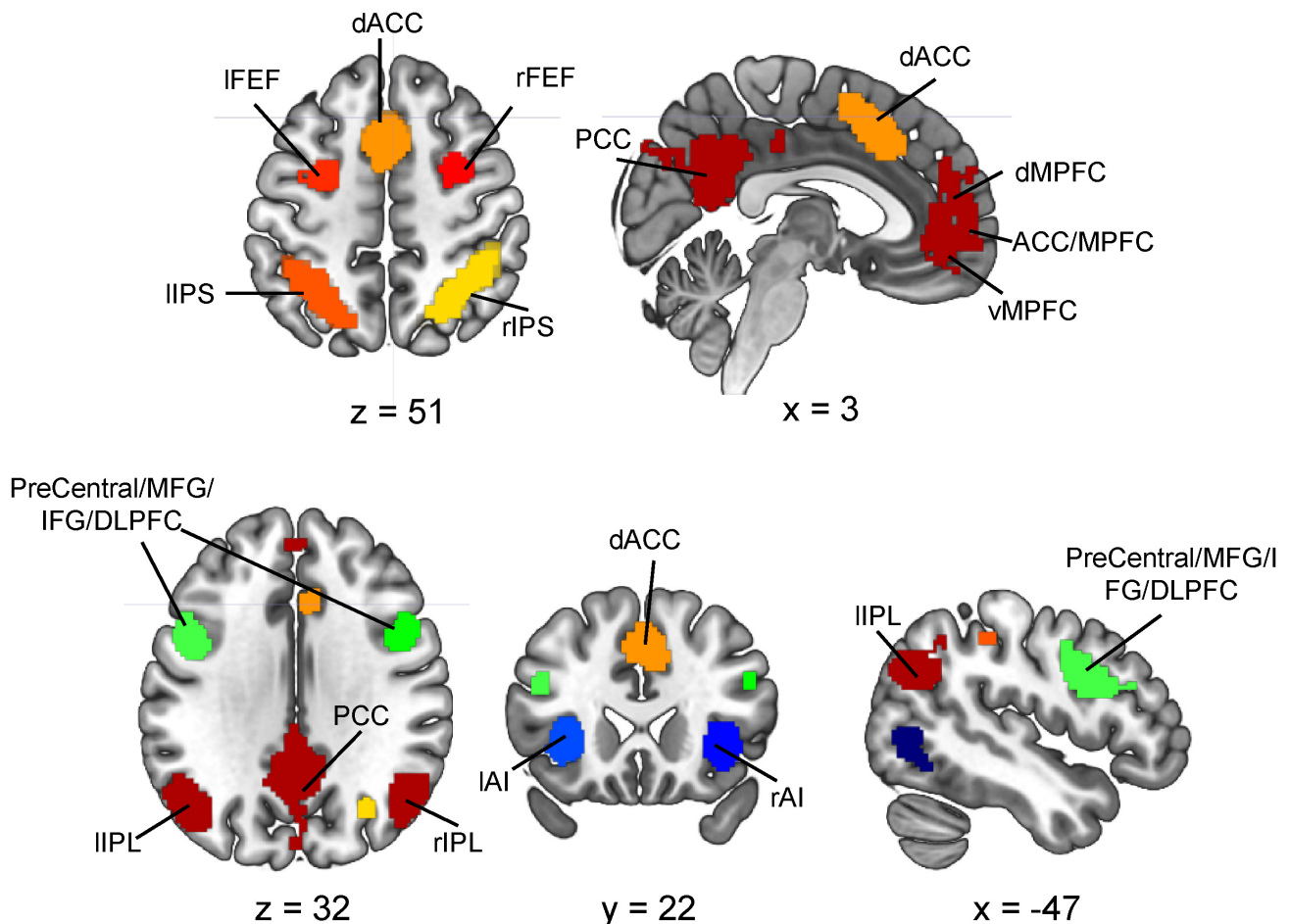


**Fig. 1.** The cognitive-control-related networks were defined based on a meta-analysis. CON, including dACC, rAI, IAI; FPN, including rFEF, IFEF, rIPS, IIPS; DMN, including MPFC, PCC, rIPL, IIPL, rLTC and ILTC; CEN, including bilateral PreCentral/MFG/IFG/DLPFC.

For the total independence (TI) and GC (Granger causality) estimations, we used the hemodynamic response function (HRF) toolbox (<http://users.ugent.be/dmarinaz/code.html>) to perform deconvolution on the preprocessed fMRI data and retrieve the signal changes at the neural level to alleviate potential confounds caused by HRF inhomogeneity [33,34].

#### 2.4 Region of Interests (ROIs) and the Connectivity Mapping

We use the Neurosynth online meta-analysis tool (<https://www.neurosynth.org>) to define the ROIs of four functional networks closely related to cognitive control, including CON, DAN, CEN, and DMN, and calculate the connectivity within CON and between CON and the rest four networks to elucidate how CON communicate with the cognitive-control-related networks (For the convenience of description, we summarized these networks as cognitive control-related functional networks (CCRN) in the current study). Specifically, the results of the meta-analysis regarding the keyword “attention” in 1831 studies provided

a well-proposed spatial pattern (uniformity test,  $p < 0.01$ , False discovery rate (FDR) corrected) of the task-positive regions of CON, DAN, and CEN. On the other hand, the results regarding the keyword “default mode” in 777 studies outlined the classical spatial pattern (uniformity test,  $p < 0.01$ , FDR corrected) of the DMN, which is thought to be a source of internal interference to goal-directed cognitive control [35]. CON ROIs included dACC and bilateral anterior insula (AI) [36]. DAN ROIs included bilateral frontal eye field (FEF) and bilateral intraparietal sulcus (IPS) [37]. CEN ROIs included bilateral precentral gyrus/frontal middle gyrus/subfrontal gyrus/dorsolateral prefrontal (PreCentral/MFG/IFG/DLPFC, collectively referred to as DLPFC in the current study [14]. DMN regions included the medial prefrontal cortex (MPFC), posterior cingulate cortex (PCC), bilateral inferior parietal lobules (IPL), and lateral temporal lobe (LTC) [38]. Please see Fig. 1 for the spatial locations of the ROIs.

The seed time series representing each CON ROI’s activity was obtained by averaging all voxel time series in that CON ROI (dACC, right AI, and left AI, respectively).

Then we calculate CC, TI, and GC between the CON ROI seed time series and each voxel of all four CCRNs (CON itself, DAN, CEN, and DMN) to yield a map that delineates the interaction between the CON ROI and other regions of CCRNs.

A common approach to demonstrate the topography is providing the thresholded T-map of an age group using a one-sample *t*-test. However, the sample size affects the *p*-value threshold selection. For age groups with different numbers of participants, setting one *p*-value threshold for all three groups is not viable for comparing their topography. Therefore, we applied a ranked mapping approach to intuitively demonstrate the difference in connectivity maps between the three age groups. Specifically, we ranked the connectivity index values across all participants for each voxel. Then we summarized that in each group, the portion of participants fell into the upper half (stronger half) of all participants. For each group, a voxel was highlighted if the portion of strong participants it represented was larger than 50%. Namely, the map illustrated whether a voxel in a given age group is strong relative to the distribution of all participants.

### 2.5 Functional Connectivity Measurement Based on Cross-Correlation

We calculated the cross-correlation [39,40] between time series to measure the FC between CON and the other four networks. The Cross-correlation (CC) is the most commonly used FC measurement describing the consistent collaboration or antagonism relationship between regions/networks. In the current study, the raw CC indices were Fisher-transformed to project the values on  $[-\infty, \infty]$ . CC measures the point-to-point linear relationship between two time series but neglects their non-zero lag temporal interdependence [32].

### 2.6 Total Interdependence

Unlike the traditional CC, total interdependence (TI) measures total temporal interdependence and accounts for the non-zero-lag relationship existing across different lags between time series (e.g., between  $x(i)$  and  $y(i+n)$ ) [32]. TI was defined by Gelfand and Yaglom [41] as:

$$TI_{x,y} = -\frac{1}{2\pi} \int_{-\pi}^{\pi} \ln(1 - C_{xy}^2(\lambda)) d\lambda \quad (1)$$

where  $C_{xy}(\lambda)$  is the coherence between the two random processes,  $x$  and  $y$ , at frequency  $f = \lambda/2\pi$ .

For a given sampling frequency  $f_s$ , the equation can be converted into an implementable form as:

$$TI_{x,y} = -\frac{2}{f_s} \sum_{i=1}^{N-1} \ln(1 - C_{xy}^2(i\Delta f)) \Delta f \quad (2)$$

where  $\Delta f$  is the frequency resolution of the spectrum of the

time series.

Therefore, by calculating TI, we can more intuitively and quantitatively prove the complete interdependence between two time series not captured by CC.

### 2.7 Granger Causality

A directed network model would be meaningful to describe the information flow between CON and the other networks. GC analysis is an effective connectivity approach useful in directed network modelling. Let  $X$  and  $Y$  be two time series, if using both  $X$ 's and  $Y$ 's past, one can predict  $Y$ 's future better than merely using  $Y$ 's past, then we say that there is GC influence from  $X$  to  $Y$  [42]. The estimation of GC is realized using the multi-variable auto-regressive (MVAR) model [43–45].

Specifically, let the two stationary time series be denoted by  $X_t$  and  $Y_t$ , each is independently represented by the following univariate autoregressive (AR) models:

$$\begin{aligned} X_t &= \sum_{j=1}^{\infty} a_{1j} X_{t-j} + \varepsilon_{1t}, \text{var}(\varepsilon_{1t}) = \Sigma_1 \\ Y_t &= \sum_{j=1}^{\infty} d_{1j} Y_{t-j} + \eta_{1t}, \text{var}(\eta_{1t}) = \Gamma_1 \end{aligned} \quad (3)$$

and jointly represented as the following bivariate AR model:

$$\begin{aligned} X_t &= \sum_{j=1}^{\infty} a_{2j} X_{t-j} + \sum_{j=1}^{\infty} b_{2j} Y_{t-j} + \varepsilon_{2t} \\ Y_t &= \sum_{j=1}^{\infty} c_{2j} X_{t-j} + \sum_{j=1}^{\infty} d_{2j} Y_{t-j} + \eta_{2t} \end{aligned} \quad (4)$$

where  $\Gamma_1$  denotes the variance of the residue of the univariate AR model fitting and  $\Gamma_2$  the covariance of the residue matrix of the bivariate (or multivariate) AR model fitting. Then GC of  $X \rightarrow Y$  can be defined as:

$$F_{X \rightarrow Y} = \ln \frac{\Gamma_1}{\Gamma_2} \quad (5)$$

According to the bayesian information criterion (BIC) and akaike information criterion (AIC) model order estimations and our previous studies [46–49], the order of the autoregressive model (AR) model was set to 2 in this study. More details of the mathematical realizations were provided in our previous study [45]. GC measures directed information flow and has been widely used in directed network modeling based on multi-unit recordings, electroencephalogram (EEG), and fMRI, providing insightful results for complex interactions among large-scale networks.

## 2.8 Connectivity-Age Correlation

We could generate connectivity maps of dACC-CCRN, rAI-CCRN, and IAI-CCRN for each participant using the above connectivity measurements. Then for each connectivity index and each CON seed ROI (say region S), we calculate the correlation coefficient between each CCRN voxel value and the age across participants to yield a map delineating the age-varying pattern of the connectivity between S and CCRNs. We start with performing the connectivity-age correlation across all participants. Further, from a lifespan perspective, it is expected that many biological indices vary in a nonmonotonic fashion against age, and taking all participants in one shot may overlook the detailed age-related pattern. It is reasonable to divide the participants according to their natural life stages and perform the correlation test in each stage. Therefore, we divided the 207 participants into three groups: Group [4–20 years old] ( $N = 56$ ), Group [21–59 years old] ( $N = 119$ ), and Group [60–85 years old] ( $N = 32$ ). The correlation analysis in Group [4–20 years old] helped to assess how the CON-CCRN interaction develops before adulthood, the analysis in Group [21–59 years old] helped to assess the changing of CON-CCRN interaction during young and middle-aged adulthood, and the analysis in Group [60–85 years old] helped to assess the changing of CON-CCRN interaction during the elder adulthood.

The connectivity-age correlation test included the following steps. First, we performed a z-transform to normalize CC, TI, and GC maps. Second, for each CCRN voxel, the correlation between each indicator and the age of participants was calculated using an age-ranked grouping method [50–53]. Specifically, (1) participants in the current age group were arranged in an age-descending order. (2) Then the analysis moved from the youngest to the eldest participant and with an increment of 1 year, and at the  $i$ th step of age  $x(i)$ , calculate the mean value of the connectivity indices  $I(i)$  and mean age  $x_{\text{mean}}(i)$  of the participants fall into the span between  $x(i)$  and  $x(i)+3$  years. (3) The correlation coefficients test between  $I$  and  $x_{\text{mean}}$  was performed to yield the correlation coefficient  $R$ , significance value  $p$ , and the coefficient of determination  $R^2$ .

## 2.9 Analysis of Variance (ANOVA)

In order to explore the difference across the three groups, we performed one-way ANOVA based on  $F$ -test for CC, TI, and GC mapping results, respectively. Statistical significance for each ANOVA was assessed at the  $p < 0.05$  level and corrected using False discovery rate (FDR) multiple comparison correction. Post hoc analysis based on the Scheffe Test was applied within the CCRN mask to reveal regions with significant changes in multiple indicators.

## 3. Result

As mentioned in the Method section, connectivity mapping results within CCRNs were correlated with age to

yield  $R$ ,  $R^2$ , and  $p$  values to describe how CON-CCRN interactions change against age. For TI and GC values, which are defined on  $[0, \infty]$ , a positive/negative  $R$  intuitively indicates an enhancement/attenuation of the connectivity indicator. Similarly, for CC between CON and DAN/CEN, which are all proposed as task-positive networks and with their activities positively correlated with each other in normal conditions, the meaning of the sign of  $R$  is the same. However, CON and DMN activities are anti-correlated in normal conditions. Therefore, if the CC of CON-DMN is positively/negatively correlated with age, that means the CON-DMN anti-correlation, is attenuated/enhanced. To keep the consistency of illuminating the enhancement and attenuation pattern, we multiplied the original  $R$  regarding the relationship of CON-DMN CC and age with  $-1$  so that positive  $R$  (after adjustment) denotes enhancement of the connection while negative  $R$  denotes attenuation.

### 3.1 The Change of CON-CCRN Interaction in All Participants

First, we use the ranked mapping approach to demonstrate the spatial difference of the connectivity map between the age groups. Noted that the classical FC was measured using cross-correlation defined on  $[-1, 1]$ , negative CC values representing anti-correlated activity could rank low, but that did not mean a weak interaction. For example, CON and DMN show prominent anti-correlation during the resting state; whether the negative correlation between CON and DMN BOLDs represents a strong but antagonist interaction or merely extremely weak coupling remains debatable. The aforementioned ranked mapping approach does not fit the complicated issue of negative FC. Therefore, we only applied the ranked mapping approach to TI and GC (Fig. 2). The result showed that the TI and GC output in Group [4–20 years old] had weaker connectivity within CON, with IIPS, and with DMN, compared to the other two groups. For GC input, CON seemed to receive more influence from DMN and IPS but less from bilateral AI.

Second, we performed ANOVA to explore the difference across the groups. No significant difference was detected across the three groups ( $p < 0.05$ , FDR correction).

Third, we performed the connectivity-age correlation across all participants. No connection indicators significantly correlate with age at a lifetime span were found ( $R^2 \geq 0.6$ ,  $p < 0.001$ ).

### 3.2 The Change of CON-CCRN Interaction in Group [2–20 Years Old]

The result showed that most of the significant connection indicators detected were positively correlated with age in this group. The detailed spatial map of the CCRN regions showed significant ( $R^2 \geq 0.6$ ,  $p < 0.001$ , FDR corrected) correlation/anti-correlation, as shown in Figs. 3,4, and with detailed information listed in Table 1. The results demonstrated several prominent patterns of the de-

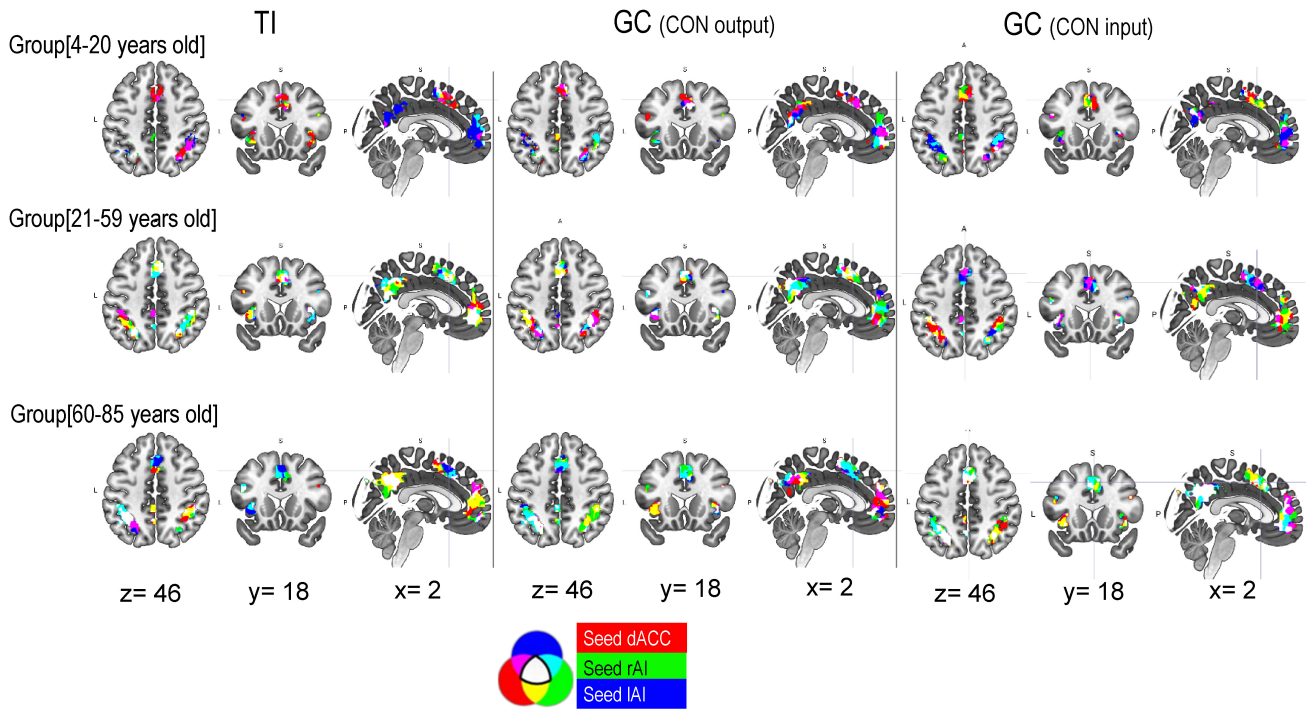


**Fig. 2. A summary of ranked seed map.** The colored regions delineate the CCRN regions that showed relatively strong connectivity with CON seed ROIs (red, seeded by dACC; green, seeded by rAI; blue, seeded by lAI).

velopment of CON-CCRN interactions. First, within the CON, enhanced CC/TI among dACC and bilateral AI and enhanced GC of dACC→ lAI/rAI and rAI→ dACC were detected, indicating increased communication within the CON from childhood to adulthood. Second, most of the indicators detected between the CON and DAN were found enhanced, such as the CC of lAI-rIPS/iIPS and rAI-rIPS/rFEF, TI of dACC-rFEF, lAI-rIPS/iIPS, and rAI-rIPS, and GC of iIPS→ lAI. Only a few indicators regarding the CON and the left DAN nodes, including the CC of dACC-iIPS, TI of rAI-lEFE, and GC of rAI→ iIPS, showed attenuation. Third, all significant connectivity indicators detected between the CON and CEN, including the CC of dACC/rAI/lAI-rDLPFC and lAI-IDLPFC, TI of dACC-rDLPFC, and GC of dACC→ rDLPFC/iDLPFC and lAI-IDLPFC, showed enhancement against age. Fourth, intense enhanced connection indicators found between the CON and DMN, including the CC of dACC-PCC/iIPL/iLTC, rAI-PCC/iIPL/rIPL, and lAI-PCC/iLTC/iIPL/rIPL/DMPFC/VMPFC/ACC, and TI of dACC-PCC/iIPL, rAI-PCC/iLTC/iIPL/rIPL, lAI-PCC/iLTC/iIPL/rIPL. Only TI: lAI/VMPFC/ACC and GC VMPFC/ACC→ lAI and rAI→ PCC showed attenuation against age. Though we set up a significant threshold of  $R^2 \geq 0.6$ , most of the enhanced indicators we detected in Group [4–20 years old] had  $R^2 \geq 0.8$ .

### 3.3 The Change of CON-CCRN Interaction in Group [21–59 Years Old]

Unlike the results of Group [4–20 years old], Group [21–59 years old] only showed a minimal number of connection indicators that showed a significant negative correlation with age. That is, within CON, the TI of lAI-dACC/rAI, and between CON and DMN, the GC of PCC→ rAI were found attenuated against age ( $0.6 \leq R^2 \leq 0.8$ ,  $p < 0.001$ , FDR corrected, see Fig. 5 and Table 2 for more details). The correlation is weaker than that of most indicators detected in Group [4–20 years old]. No significant positive correlations were detected between the connection indicators and age.

### 3.4 The Change of CON-CCRN Interaction in Group [60–85 Years Old]

The results of Group [60–85 years old] (Fig. 6, Table 3) showed an inversed pattern compared to that of Group [4–20 years old]. Most of the connection indicators detected ( $R^2 \geq 0.6$ ,  $p < 0.001$ , FDR corrected) showed attenuation against age, distributed within CON and between CON and DMN. Within CON, the CC and TI of lAI/rAI-dACC were found significantly attenuated. Between CON and DMN, the CC of dACC/rAI-PCC, dACC/lAI-rIPL, lAI-VMPFC/ACC, and dACC-DMPFC/VMPFC/ACC, TI of dACC/lAI-PCC, and GC of lAI→ iIPL were found significantly attenuated. Only the TI of lAI-rIPS was found to be enhanced.

**Table 1. CON-CCRN connections significantly correlated with age in Group [4–20 years old].**

Connectivity Index_Seed ROI	[Network]-ROI	MNI coordinate			Sign of <i>R</i>	<i>R</i>	<i>R</i> <sup>2</sup>	<i>p</i> (FDR)
		x	y	z				
TI_Seed_rAI	[CON]-dACC	3	26	32	+	0.91	0.83	<0.001
TI_Seed_rAI	[CON]-dACC	0	23	50	+	0.93	0.86	<0.001
CC_Seed_rAI	[CON]-dACC	3	26	32	+	0.93	0.86	<0.001
CC_Seed_IAI	[CON]-dACC	9	17	38	+	0.94	0.89	<0.001
TI_Seed_dACC	[CON]-IAI	-30	26	-4	+	0.96	0.93	<0.001
TI_Seed_rAI	[CON]-IAI	-39	17	-7	+	0.89	0.79	<0.001
GC_Output_Seed_dACC	[CON]-IAI	-36	26	5	+	0.93	0.87	<0.001
CC_Seed_dACC	[CON]-IAI	-36	20	-7	+	0.96	0.92	<0.001
CC_Seed_rAI	[CON]-IAI	-33	17	2	+	0.90	0.8	<0.001
TI_Seed_dACC	[CON]-rAI	33	20	2	+	0.96	0.92	<0.001
TI_Seed_IAI	[CON]-rAI	33	29	-1	+	0.97	0.94	<0.001
GC_Output_Seed_dACC	[CON]-rAI	36	20	8	+	0.96	0.93	<0.001
GC_Input_Seed_dACC	[CON]-rAI	39	17	-4	+	0.98	0.96	<0.001
CC_Seed_dACC	[CON]-rAI	39	20	-7	+	0.97	0.94	<0.001
CC_Seed_IAI	[CON]-rAI	33	29	-4	+	0.96	0.91	<0.001
TI_Seed_rAI	[DAN]-IFEF	-24	-7	56	-	-0.91	0.82	<0.001
TI_Seed_IAI	[DAN]-IIPS	-30	-55	44	+	0.97	0.94	<0.001
GC_Output_Seed_rAI	[DAN]-IIPS	-39	-37	41	-	-0.94	0.89	<0.001
GC_Input_Seed_IAI	[DAN]-IIPS	-42	-46	53	+	0.97	0.94	<0.001
CC_Seed_dACC	[DAN]-IIPS	-27	-52	50	-	-0.95	0.91	<0.001
CC_Seed_IAI	[DAN]-IIPS	-39	-40	41	+	0.97	0.94	<0.001
CC_Seed_IAI	[DAN]-IIPS	-18	-67	56	+	0.96	0.92	<0.001
TI_Seed_dACC	[DAN]-rFEF	33	-1	56	+	0.95	0.9	<0.001
CC_Seed_rAI	[DAN]-rFEF	24	-1	56	+	0.93	0.87	<0.001
TI_Seed_rAI	[DAN]-rIPS	48	-37	44	+	0.99	0.97	<0.001
TI_Seed_IAI	[DAN]-rIPS	48	-37	44	+	0.97	0.95	<0.001
CC_Seed_rAI	[DAN]-rIPS	48	-40	47	+	0.95	0.9	<0.001
CC_Seed_IAI	[DAN]-rIPS	45	-40	47	+	0.97	0.94	<0.001
TI_Seed_dACC	[CEN]-IFG	48	11	20	+	0.98	0.96	<0.001
GC_Output_Seed_dACC	[CEN]-IFrontal_Inf_Tri	-48	20	29	+	0.94	0.89	<0.001
GC_Output_Seed_dACC	[CEN]-IMFG/DLPFC	-45	20	23	+	0.90	0.81	<0.001
GC_Output_Seed_IAI	[CEN]-IPreCentral	-42	-1	38	+	0.93	0.86	<0.001
CC_Seed_IAI	[CEN]-IPreCentral	-39	5	35	+	0.91	0.82	<0.001
CC_Seed_dACC	[CEN]-rFrontal_Inf_Oper/rpMFG	51	5	41	+	0.96	0.91	<0.001
CC_Seed_IAI	[CEN]-rFrontal_Inf_Oper/rpMFG	54	14	23	+	0.94	0.88	<0.001
GC_Output_Seed_dACC	[CEN]-rFrontal_Inf_Tri	45	26	26	+	0.96	0.91	<0.001
GC_Output_Seed_dACC	[CEN]-rMFG/DLPFC	45	35	23	+	0.91	0.84	<0.001
TI_Seed_dACC	[CEN]-rPreCentral	48	2	38	+	0.98	0.96	<0.001
CC_Seed_rAI	[CEN]-rPreCentral	51	5	38	+	0.97	0.95	<0.001
CC_Seed_IAI	[CEN]-rPreCentral	45	5	38	+	0.98	0.97	<0.001
TI_Seed_dACC	[DMN]-IIPPL	-51	-61	26	+	0.93	0.87	<0.001
TI_Seed_rAI	[DMN]-IIPPL	-42	-64	26	+	0.90	0.81	<0.001
TI_Seed_IAI	[DMN]-IIPPL	-42	-70	26	+	0.95	0.9	<0.001
CC_Seed_dACC	[DMN]-IIPPL	-45	-67	35	+	0.94	0.89	<0.001
CC_Seed_rAI	[DMN]-IIPPL	-42	-64	35	+	0.95	0.91	<0.001
CC_Seed_IAI	[DMN]-IIPPL	-45	-64	35	+	0.97	0.94	<0.001
TI_Seed_rAI	[DMN]-ILTC	-66	-16	-16	+	0.90	0.82	<0.001
TI_Seed_IAI	[DMN]-ILTC	-66	-19	-19	+	0.91	0.83	<0.001
CC_Seed_dACC	[DMN]-ILTC	-63	-22	-16	+	0.96	0.92	<0.001

**Table 1. Continued.**

Connectivity Index_Seed ROI	[Network]-ROI	MNI coordinate			Sign of <i>R</i>	<i>R</i>	<i>R</i> <sup>2</sup>	<i>p</i> (FDR)
		x	y	z				
CC_Seed_IAI	[DMN]-ILTC	-57	-19	-16	+	0.94	0.89	<0.001
CC_Seed_5_rAI	[DMN]-MPFC	-6	53	8	+	0.93	0.86	<0.001
TI_Seed_rAI	[DMN]-vMPFC	-3	53	-13	+	0.95	0.91	<0.001
TI_Seed_IAI	[DMN]-vMPFC/ACC	-9	50	8	-	-0.86	0.74	<0.001
GC_Input_Seed_IAI	[DMN]-vMPFC/ACC	6	41	-4	-	-0.95	0.91	<0.001
CC_Seed_rAI	[DMN]-vMPFC	3	50	2	+	0.95	0.9	<0.001
CC_Seed_IAI	[DMN]-vMPFC	-6	50	-13	+	0.97	0.94	<0.001
CC_Seed_IAI	[DMN]-vMPFC	0	59	2	+	0.97	0.95	<0.001
TI_Seed_dACC	[DMN]-PCC	0	-49	32	+	0.85	0.72	<0.001
TI_Seed_rAI	[DMN]-PCC	0	-52	32	+	0.96	0.93	<0.001
TI_Seed_IAI	[DMN]-PCC	-3	-52	17	+	0.98	0.97	<0.001
GC_Output_Seed_rAI	[DMN]-PCC	9	-58	20	-	-0.92	0.85	<0.001
GC_Input_Seed_IAI	[DMN]-PCC	-3	-58	14	-	-0.94	0.89	<0.001
CC_Seed_dACC	[DMN]-PCC	-3	-52	32	+	0.95	0.89	<0.001
CC_Seed_rAI	[DMN]-PCC	-6	-52	17	+	0.97	0.94	<0.001
CC_Seed_rAI	[DMN]-PCC	-6	-55	38	+	0.94	0.88	<0.001
CC_Seed_IAI	[DMN]-PCC	6	-43	35	+	0.97	0.94	<0.001
CC_Seed_IAI	[DMN]-dMPFC	3	53	17	+	0.9	0.81	<0.001
TI_Seed_rAI	[DMN]-rIPL	54	-58	23	+	0.97	0.93	<0.001
TI_Seed_IAI	[DMN]-rIPL	45	-58	26	+	0.88	0.78	<0.001
CC_Seed_rAI	[DMN]-rIPL	51	-61	35	+	0.96	0.92	<0.001
CC_Seed_IAI	[DMN]-rIPL	54	-58	38	+	0.93	0.87	<0.001

Note: The sign of “+”/“-” denotes a significant positive/negative correlation between age and connection strength. CC, cross-correlation; TI, total interdependence; GC\_Output, Granger causality from the CON seed ROI to others; GC\_Input, Granger causality of the CON seed ROI received from others; CON, cingulo-opercular network; DAN, dorsal attention network; CEN, central executive network; DMN, default mode network; dACC, dorsal anterior cingulate cortex; rAI/lAI, right/left anterior insula; lIPS/rIPS, left/right intraparietal sulcus; lFEF/rFEF, left/right frontal eye field; lIPL/rIPL, left/right parietal lobe; ILTC/rLTC, left/right lateral temporal cortex; VMPFC, ventromedial prefrontal cortex; MPFC/ACC, medial prefrontal/anterior cingulate cortex; PCC, posterior cingulate cortex; DMPFC, dorsomedial prefrontal cortex; IFG, inferior frontal gyrus; lFrontal\_Inf\_Tri/rFrontal\_Inf\_Tri, left/right triangular inferior frontal gyrus; l/rMFG/DLPFC, left/right middle frontal gyrus/dorsolateral prefrontal cortex; l/rPreCentral, left/right precentral gyrus; rFrontal\_Inf\_Oper /rpMFG, inferior frontal gyrus of right insular operculum/posterior middle frontal gyrus.

**Table 2. CON-CCRN connections significantly correlated with age in Group [21–59 years old].**

Connectivity Index_Seed ROI	[Network]-ROI	MNI coordinate			Sign of <i>R</i>	<i>R</i>	<i>R</i> <sup>2</sup>	<i>p</i> (FDR)
		x	y	z				
TI_Seed_IAI	[CON]-rAI	33	20	-4	-	-0.78	0.62	<0.001
TI_Seed_IAI	[CON]-rAI	33	23	5	-	-0.80	0.64	<0.001
TI_Seed_IAI	[CON]-dACC	9	23	35	-	-0.87	0.76	<0.001
TI_Seed_IAI	[CON]-dACC	-3	20	47	-	-0.84	0.7	<0.001
GC_Input_Seed_rAI	[DMN]-PCC	0	-40	32	-	-0.83	0.68	<0.001

Conventions are the same as those in Table 1.

## 4. Discussion

The current study adopted a multi-connectivity indicator-based network analysis approach to explore the lifelong changes in functional and effective connectivity within CON and between CON and several cognitive control-related functional networks (DAN, DMN, and

CEN) from age 4–85 years. We found three major results. (1) The connectivity indices within the CON and between CON and the other three CCRNs showed significant enhancement from childhood to early adulthood (age 4–20 years), (2) mild attenuation within CON from early adulthood to middle age (age 21–59 years), and (3) significant

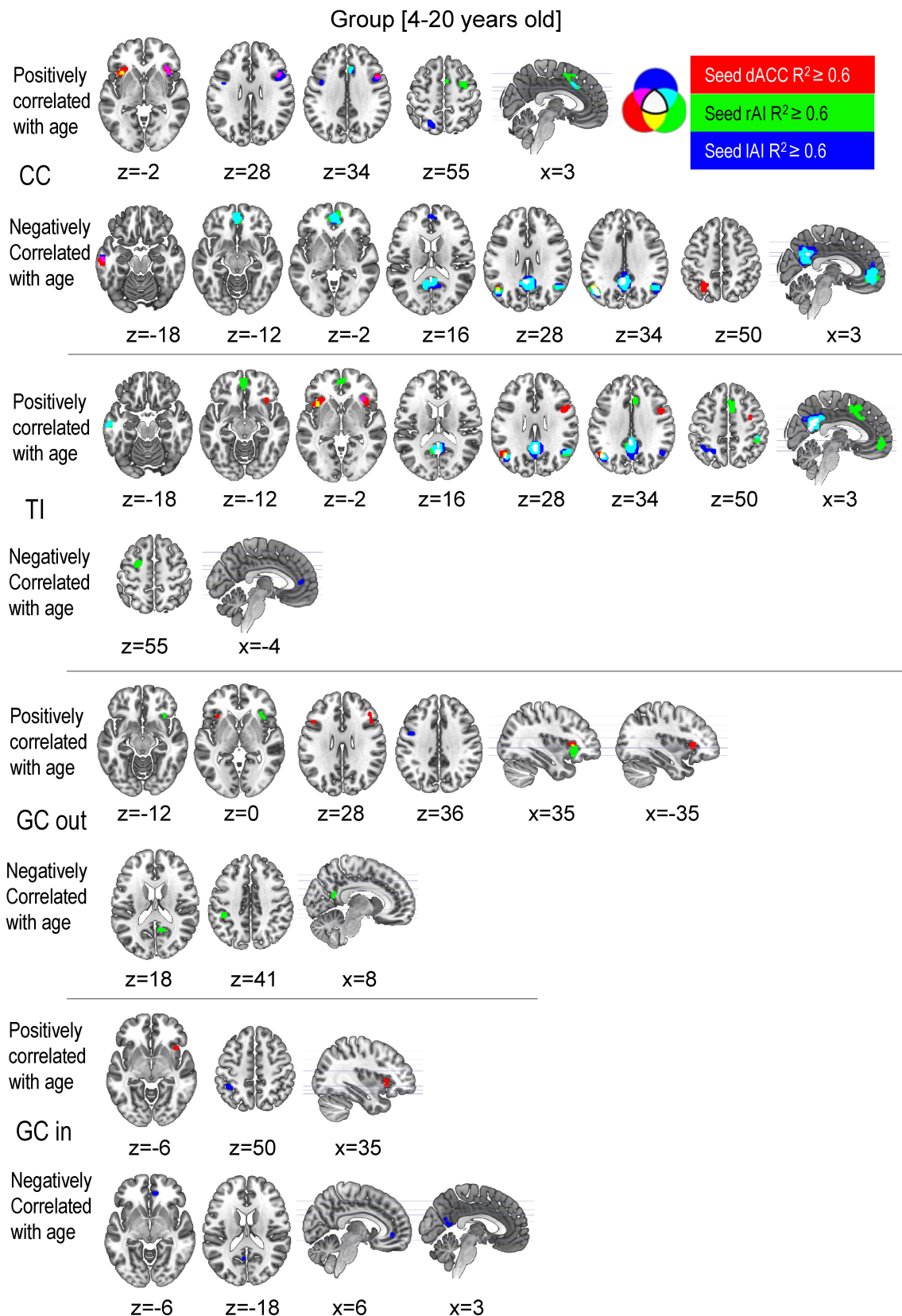


**Fig. 3. CCRNs connectivity changed against age in Group [4-20 years old].** The colored CCRN regions show significant correlations ( $R^2 \geq 0.6$ ,  $p < 0.001$ , cluster size  $> 20$  voxels) between the connectivity indices with age in Group [4-20 years old]. The color schema is the same as that in Fig. 2.

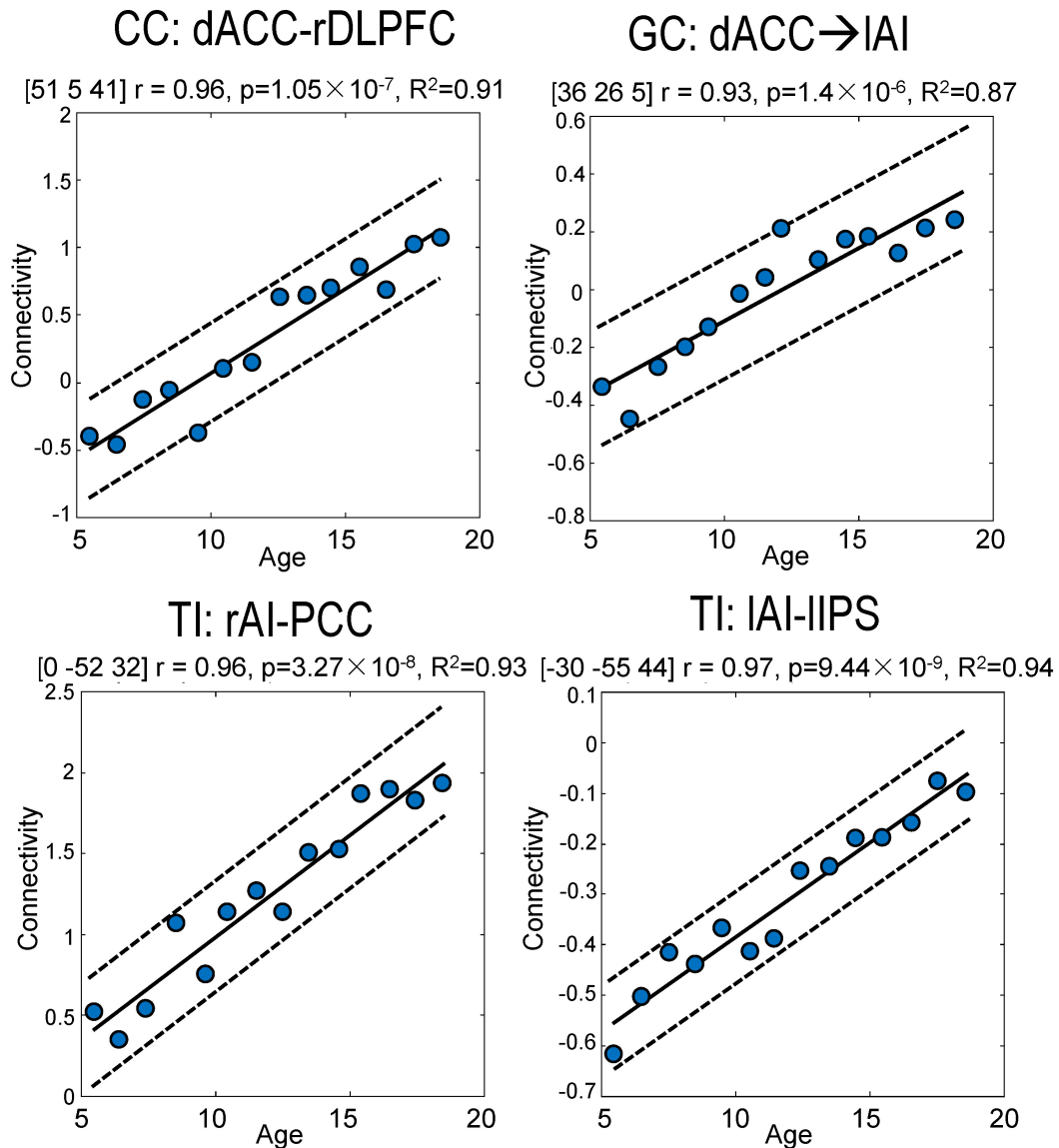


Fig. 4. Examples of the scatter plot of the connectivity index correlated with age in Group [4–20 years old].

attenuation within CON and between CON and DMN in the elder group (age 60–85 years). The main pattern of the changes is schematically summarized in Fig. 7. The current study aimed to characterize the changing pattern of the interactions between CON and several well-proposed functional networks (including CON itself) that are closely associated with cognitive control at different stages of life.

#### 4.1 CON-CCRN Connectivity Change across Different Age Stages

Although the ranked mapping result showed some trend of change across different age groups, the ANOVA results did not reveal significant change between the age groups. Four points may explain why no significant re-

sults were disclosed using ANOVA: (1) The Group [4–20 years old] and Group [59–85 years old] belong to the two populations that were experiencing significant changes in their brain functional connectivity. For example, the Group [4–20 years old] covered participants from preschoolers, schoolchildren, preteens, teenagers, and even early young adults. It was not surprising that the variance of the connectivity indicators contributed by the developmental effect in this group was large. Similarly, the Group [59–85 years old] might also have a large variance contributed by aging. (2) The individual difference in functional connectivity also contributed much to the variance besides the age in all three groups. (3) The variance caused by the two effects mentioned above blurred the boundary of two neighboring

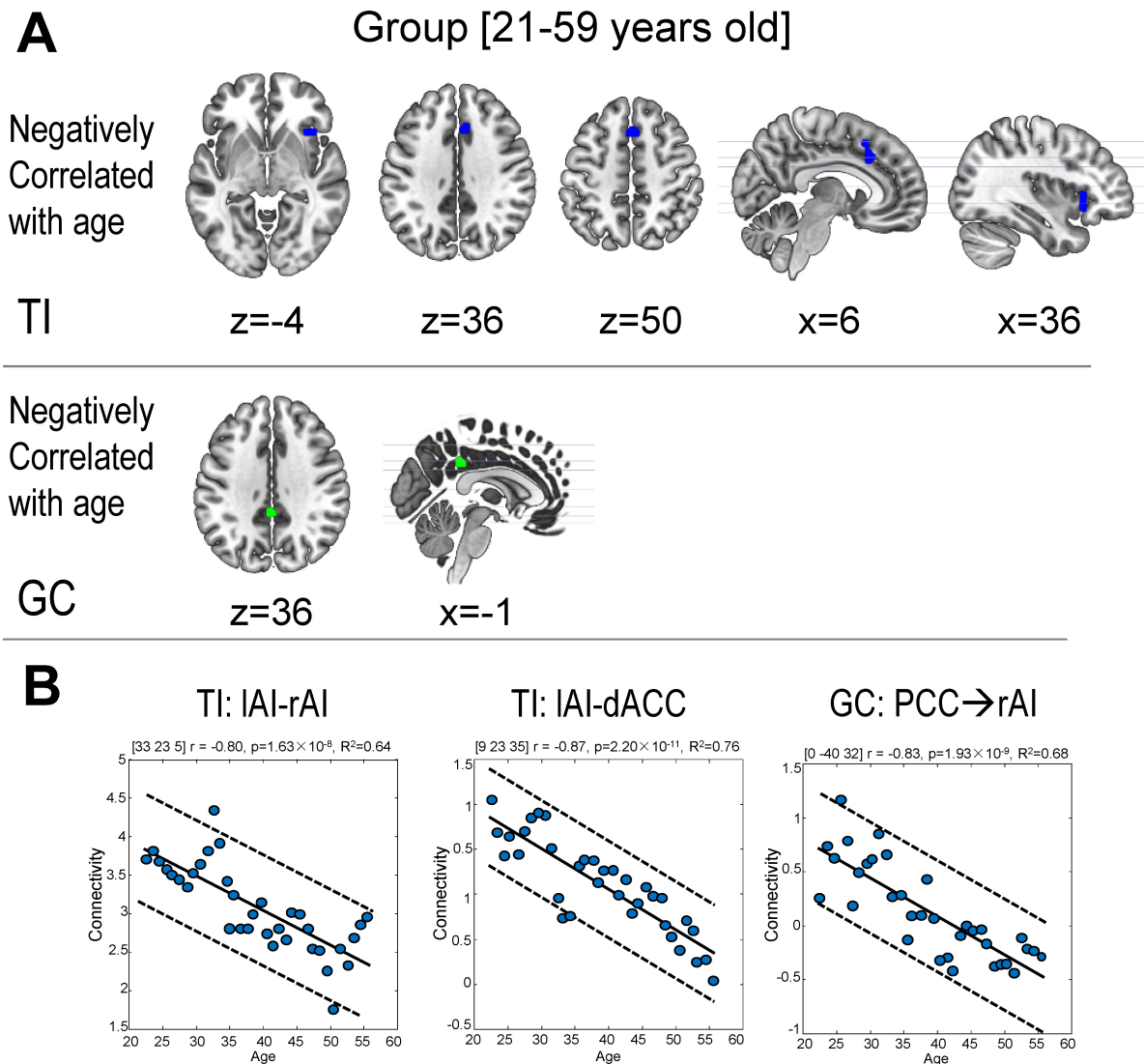


**Fig. 5. CCRNs connectivity changed against age in Group [21–59 years old].** (A) CCRNs regions show significant correlations ( $R^2 \geq 0.6$ ,  $p < 0.001$ , cluster size  $> 20$  voxels) between the connectivity indices with age in Group [21–59 years old]. (B) demonstrates examples of the scatter plot of the connectivity index correlated with age. The color schema is the same as that in Fig. 3.

groups, making detecting group differences difficult. (4) If the change was not monotonic, it was possible that few significant changes could be detected across groups. For example, if the connectivity increased with age in Group [4–20 years old] but decreased with age in Group [59–85 years old], the connectivity might show no change across the two groups. In summary, for the dataset analyzed in the current study, compared with correlation analysis, ANOVA might not capture the detailed alteration pattern across the groups. The null results of ANOVA indicated that dividing the participants into age groups and analyzing how CON-CCRN interaction changes with age within each Group is necessary.

#### 4.2 CON-CCRN Connectivity Change at a Lifetime Scale

Although the results of including all participants in the connectivity-age correlation analysis were insignificant, they also showed that it was necessary to divide the participants into different age stages, calculate the correlation within each stage, and summarize the changing pattern of a lifetime. A few points are worth discussing here:

(1) Including participants of all age groups, the number of samples increased, and the p-value might decrease. However, when examining the correlation with age, both  $R$  and  $R^2$  showed a significant decline, which showed that on a lifelong scale, the changes of most connectivity indicators were probably not linear, and each age stage has its change pattern, which demands the analysis strategy of ex-

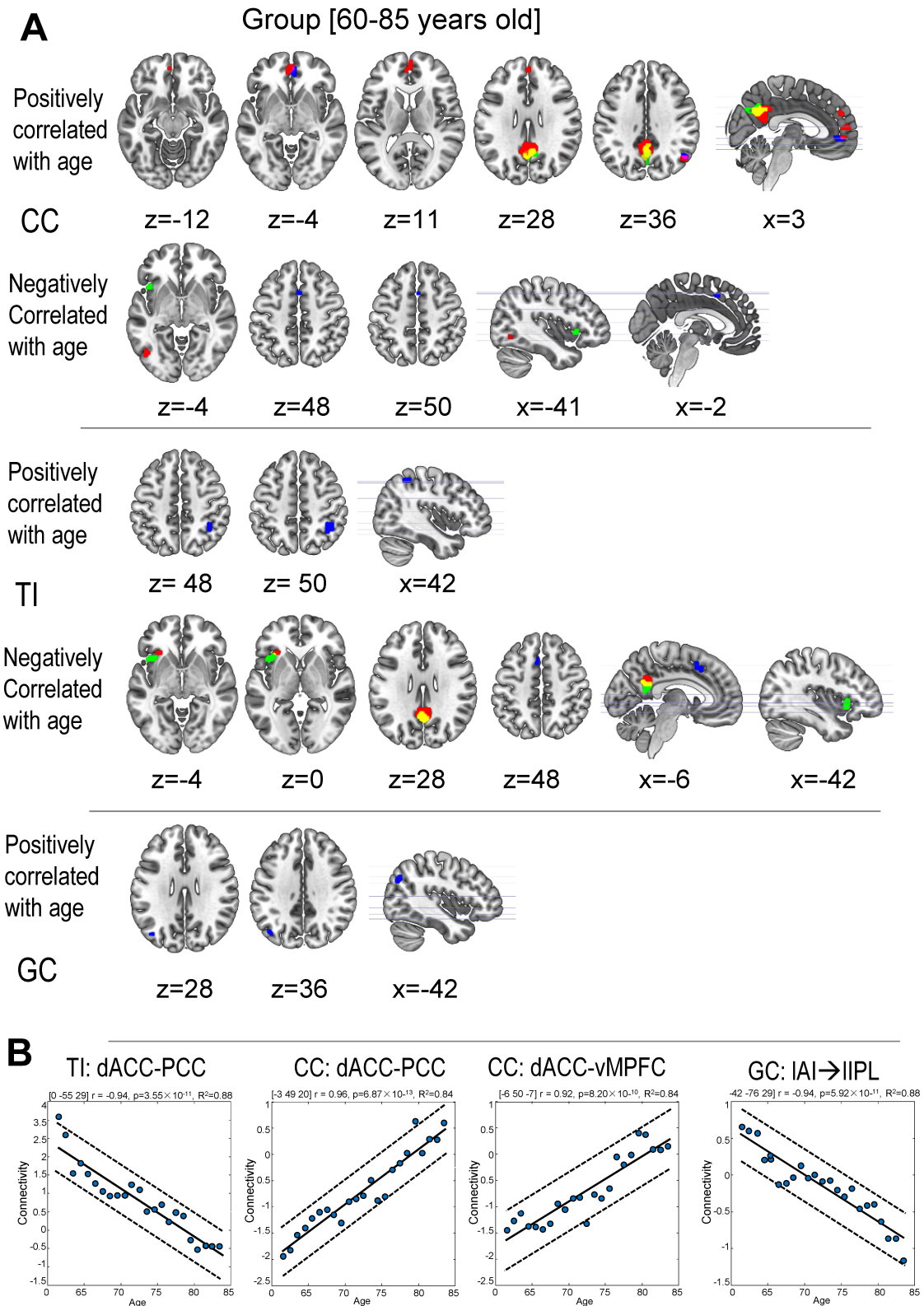


**Fig. 6. CCRNs connectivity changed against age in Group [60–85 years old].** (A) CCRNs regions show significant correlations ( $R^2 \geq 0.6$ ,  $p < 0.001$ , cluster size  $> 20$  voxels) between the connectivity indices with age in Group [60–85 years old]. (B) demonstrates examples of the scatter plot of the connectivity index correlated with age. The color schema is the same as that in Fig. 3.

**Table 3. CON-CCRN connections significantly correlated with age in Group [60–85 years old].**

Connectivity Index_Seed ROI	[Network]-ROI	MNI coordinate			Sign of $R$	$R$	$R^2$	$p$ (FDR)
		x	y	z				
TI_Seed_lAI	[CON]-dACC	-6	20	41	-	-0.91	0.82	<0.001
CC_Seed_lAI	[CON]-dACC	-3	14	44	-	-0.91	0.83	<0.001
TI_Seed_dACC	[CON]-lAI	-27	26	-1	-	-0.94	0.87	<0.001
TI_Seed_rAI	[CON]-lAI	-39	20	2	-	-0.98	0.96	<0.001
CC_Seed_rAI	[CON]-lAI	-45	17	-1	-	-0.97	0.93	<0.001
TI_Seed_lAI	[DAN]-rIPS	36	-46	50	+	0.90	0.81	<0.001
CC_Seed_dACC	[DMN]-ACC/MPFC	-6	47	11	-	-0.84	0.71	<0.001
CC_Seed_lAI	[DMN]-ACC/vMPFC	6	41	-1	-	-0.90	0.81	<0.001
CC_Seed_dACC	[DMN]-dMPFC	-3	47	32	-	-0.90	0.81	<0.001
CC_Seed_dACC	[DMN]-dMPFC	3	50	32	-	-0.90	0.80	<0.001
CC_Seed_dACC	[DMN]-dMPFC	3	56	14	-	-0.91	0.82	<0.001
GC_Output_Seed_lAI	[DMN]-I IPL	-42	-76	29	-	-0.94	0.88	<0.001
CC_Seed_dACC	[DMN]-vMPFC	-6	50	-7	-	-0.92	0.84	<0.001
CC_Seed_lAI	[DMN]-vMPFC	6	53	-7	-	-0.90	0.81	<0.001
CC_Seed_dACC	[DMN]-MPFC	3	47	26	-	-0.91	0.82	<0.001
CC_Seed_dACC	[DMN]-MPFC	0	56	-4	-	-0.92	0.85	<0.001
TI_Seed_dACC	[DMN]-PCC	0	-55	29	-	-0.94	0.88	<0.001
TI_Seed_rAI	[DMN]-PCC	-3	-49	17	-	-0.94	0.89	<0.001
CC_Seed_dACC	[DMN]-PCC	-3	-49	20	-	-0.96	0.92	<0.001
CC_Seed_rAI	[DMN]-PCC	9	-58	26	-	-0.93	0.86	<0.001
CC_Seed_dACC	[DMN]-rIPL	42	-58	32	-	-0.85	0.72	<0.001
CC_Seed_dACC	[DMN]-rIPL	51	-67	35	-	-0.85	0.71	<0.001
CC_Seed_lAI	[DMN]-rIPL	54	-64	35	-	-0.88	0.77	<0.001

Conventions are the same as those in Table 2.

aming within age groups. Our results also explained this point. For example, Group [21–59 years old] had the largest sample number ( $N = 119$ ) and the largest age span, but the number of brain regions with changed connectivity significantly correlated with age was minimum, indicating that the connection between CON and CCRN regions is stable, and generally does not change significantly with age. When analyzing the whole cohort, participants aged 21–59 might be dominant in the sample size and age span. Therefore, it was likely that the details of network connection change of the other two age groups would be lost.

(2) Existing studies have shown that the trend of brain connection changes in the three age groups is very inconsistent. The meaning of using linear correlation to explore possible general change patterns at a lifetime scale from a data-driven perspective needs to be clarified.

(3) Although the results were insignificant regarding the criteria we applied in the current study, providing the so-called “null results” were still helpful. In the current study, it is reasonable to start with a correlation analysis across the whole cohort. The “negative results” of the whole cohort correlation analysis, like the “negative results” of ANOVA, provided insight into the reason for performing correlation analysis within each age group and enhanced the motivation

of the analysis strategy applied in the current study.

#### 4.3 The Integration and Disintegration of CON at Different Age Stages

Two of the main results of the current study were that the connections between the CON regions (dACC and bilateral AI) showed significant enhancement against age before adulthood but showed attenuation during aging in adulthood. The former suggested increased integration between nodes within CON, indicating a typical pattern of CON development at the age of 4–20 years, which is consistent with the previous study [54]. According to previous research [55], this integration may be related to the central regulatory role of CON among the large-scale functional networks [4,12,13,56,57]. The result also showed that the connectivity enhancement of dACC-lAI/rAI is more prominent than that of lAI-rAI, indicating a core position of dACC in the development of the hierarchy of CON node, which was in line with our previous findings that dACC is on a higher level than AI in control [52,53]. On the other hand, in Group [4–20 years old], the enhancement of dACC-rAI connections seemed to be more significant than those of the other connections in CON. For example, the  $R^2$  of the correlation between rAI  $\rightarrow$  dACC and age reached 0.96, the largest  $R^2$

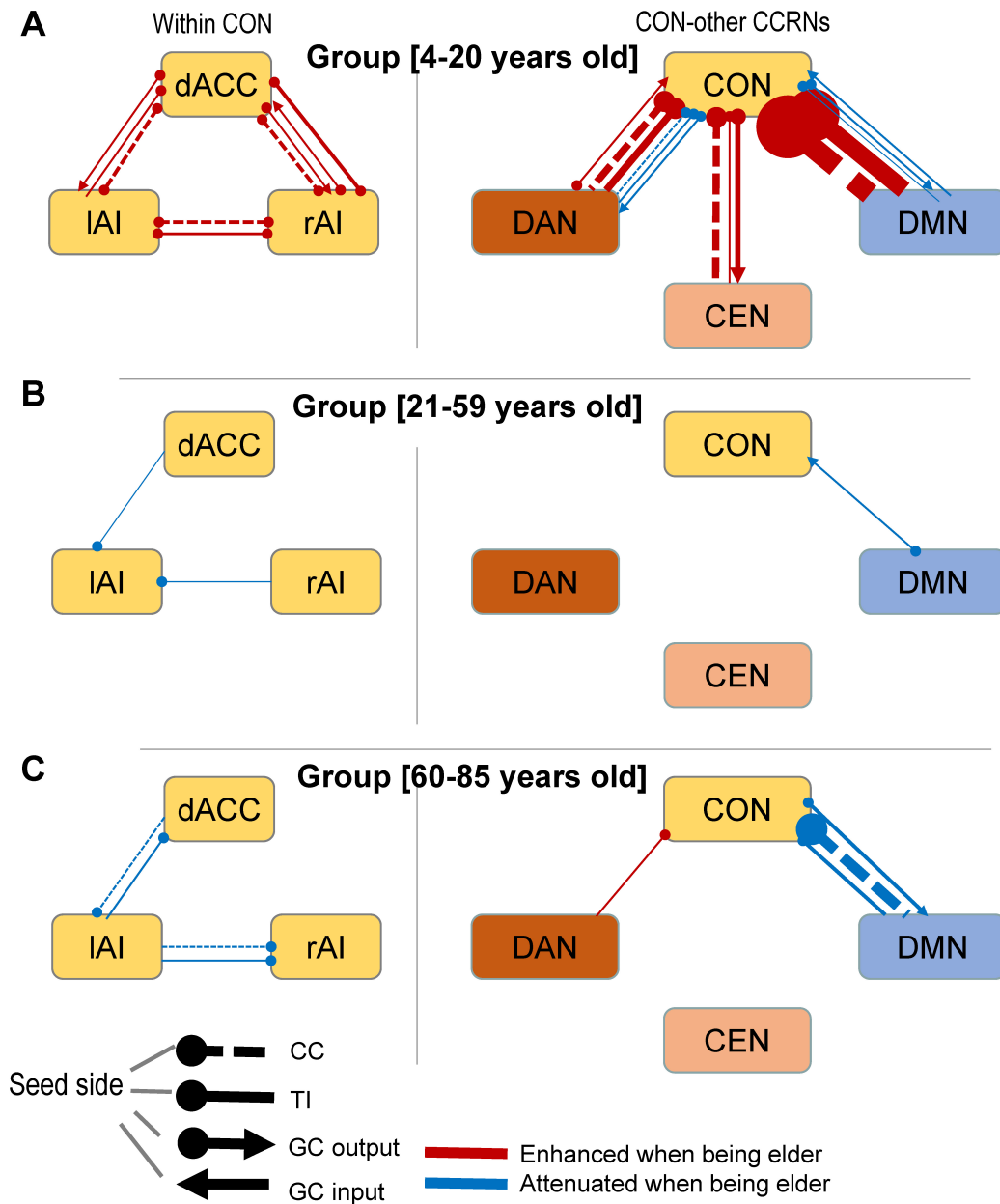


**Fig. 7. A schematic summary of the significantly enhanced/attenuated CON-CCRNs connection indicators in different age groups.** (A) Change pattern in Group [4–20 years old]. (B) Change pattern in Group [21–59 years old]. (C) Change pattern in Group [60–85 years old]. The weights of the connections are proportional to the number of indicators that were significantly correlated with age.

among the connections within CON. This result supports the view of the Triple Network Regulation Model that the rAI is central to the dynamic regulation of functional networks [13,58]. It is worth noting that the ventral AI area showed significantly enhanced FC. In contrast, dorsal AI showed enhanced GC. This discrepant pattern was consistent with previous findings that ventral AI is more associated with emotional processing, and the dorsal side is more associated with higher-order cognitive processes [58–60]. These results suggest that the dorsal and ventral of AI undergo functional differentiation and integration into different subnetworks during development.

In both Groups with ages over 20, we observed attenuation of TI of dACC-IAI and rAI-IAI. The attenuation is mild and only showed in TI indicators when participants are younger than 60 (Group [21–59 years old]). For participants over 60 (Group [60–85 years old]), the attenuation became more significant in both CC and TI indicators. The mild attenuation from early adulthood to late middle age may reflect an early sign of the decline of CON. The more severe attenuation in participants over 60 reflects the consequence of the early decline. It is worth noting that the connection indicators between dACC and rAI, though prominently enhanced before 20 years old, did not show

significant change during aging. This result indicated that the interaction between dACC and rAI might be a binding signature of developing the cognitive control functions in younger participants and maintaining them in the older participants under normal conditions. The varying pattern of dACC-rAI interaction implies that its abnormal alteration may be associated with a mental illness involving impaired cognitive control [61]. This needs further investigation beyond the normal population.

#### 4.4 Enhanced Integration between CON and CEN, and DAN in Development

Task-positive networks such as CON, DAN, and CEN play a crucial role in the performance of cognitive tasks. Dosenbach *et al.* [56] suggested that the CON served as the regulatory core of the task-positive network, monitoring the CEN and DAN, which were involved in specific task trials. The present study found that the coupling between CON and DAN/CEN increased with age during development, which is consistent with some previous findings which demonstrated a gradual increase in FC between CON and the DAN/CEN [23,62] from childhood to adulthood. This enhancement has been proposed to be critical for cognitive control maturity [24]. In addition, GC indicators further revealed the stronger influence of rAI → IDLPFC, dACC → r/IDLPFC, and IIPS → LAI but weakened the influence of rAI → IIPS. Sridharan *et al.* [13] argued that the rAI, as the main site of stimulus reception/response, is first activated upon receipt of external stimuli and subsequently generates priming to activate the dACC, LAI to trigger hierarchical control. DLPFC and IPS are involved in top-down control of cognitive control signals at the sub-trial level of the task. The present study only found GC influence of LAI/dACC → DLPFC but not the rAI → DLPFC, and enhanced interaction between the LAI and IPS but a weakened interaction between the right AI and IPS during development, which may indirectly support the hypothesis that right AI regarding initiation.

Taken together, the enhanced coupling, total interdependence, and directional GC influence between CON and DAN/CEN before adulthood delineated a procedure of developmental maturation characterized by the integration of the so-called task-positive networks, including CON, DAN, and CEN.

#### 4.5 Stable Pattern of CON-CCRN's Interaction from Early Adulthood to Middle Age

In Group [21–59 years old], only a small number of connection indicators correlated with age. The scatter plot of most connection indices did not show a significant pattern of increasing or decreasing or nonlinear trends against age, despite this Group containing the largest number of participants ( $n = 119$ ) in the current study. The result indicated that most of the CON-CCRN's connections do not change significantly or systematically against age and en-

ter a stable stage after adolescence. The negative results of most connections may be a sign of matured CON-CCRN's integration and are in line with the proposed trend of cognitive control in humans [55,63,64]. On the other hand, disentangled CON-CCRN's interaction may impair emotional and cognitive functions. For example, previous research has reported altered connections of CON-CCRN's in psychiatric disorders such as depression [65], anxiety [66], and Alzheimer's disease [67]. This stable stage could also be critical to maintaining normal functions in adulthood.

#### 4.6 CON-DMN Communication Change Against Age

The enhancement during the development and the attenuation of CON-DMN connection indicators were the most noticeable results we observed in the current study (Fig. 7). DMN is well-known as a task-negative network constantly deactivated when an individual performs cognitively demanding tasks and shows more active signal change when the task is absent [38,68–71]. DMN is thought to be associated with mind wandering and free thinking and the source of internal interference to the external goal-directed task performance [38,52]. The regulation of DMN during a task is important for many behaviors that demand cognitive control, such as attention [52,72], working memory [73,74], meditation [69], etc. The attenuated deactivation of DMN during cognitive tasks has been reported constantly in elders, patients with mild cognitive impairment (MCI) [75], patients with Alzheimer's Disease [76], Children with attention deficit, and other developmental problems [77,78]. Previous studies have suggested that effective CON-DMN communication is crucial for successfully regulating DMN activity during cognitive control [52,79]. The antagonistic relationship (measured using anti-correlation [40]) between CON and DMN activity is a sign of effective communication both during the task and during the resting state.

In the current study, the CC indicator showed enhanced anti-correlation between CON-DMN in Group [4–20 years old], indicating increased communication from childhood to adulthood. Consistently, the TI of CON-DMN also showed enhancement against age in Group [4–20 years old], which confirmed the increased CON-DMN communication. This developing pattern of CON-DMN interaction may suggest a balance of internal and information processing and be related to the functional development and improvement of individual functional networks to cope with more complex cognitive tasks when children and adolescents grow up [76,80].

On the other hand, the results in Group [60–85 years old] showed significant attenuation of the CON-DMN interaction in elder participants. For example, the anti-correlation measured in CC between many CON and DMN nodes was significantly weakened against age. Consistently, for dACC and rAI, two major nodes of CON, and PCC, a representative hub of DMN, the TI of dACC/rAI-

PCC were also significantly weakened when participants' age became older. The result showed a pattern contrary to that in the children and young group. This attenuation in CON-DMN interaction may underlie the neural basis of the decline in cognitive function during aging [81]. The attenuation was not observed in the connection indicators of CON-DAN/CEN, indicating that cognitive decline during aging is mainly related to the disrupted communication between CON and DMN instead of those between the task-positive CCRNs [81]. The attenuation was not observed in the connection indicators of CON-DAN/CEN, indicating that cognitive decline during aging is mainly related to the disrupted communication between CON and DMN instead of those between the task-positive CCRNs.

#### 4.7 Considerations and Limitations

Although there are many studies on the change of functional connectivity with age, only a small number of studies [22] focused on how the connectivity of CON and CCRNs changes in a lifetime and support the proposed core control network theory [9]. However, the previous research has the following limitations. (1) It was only based on a single FC indicator using cross-correlation and could not provide directional information. (2) It performed correlation analysis across participants of all ages and only examined the relationship of linear, monotonic changes, ignoring that the change of CON-CCRN communication in a lifetime could be nonmonotonic.

Therefore, as an essential core cognitive control network, the changing communication pattern between CON and other CCRNs needs to be clarified. This study can be regarded as a follow-up study of the previous work examining the interaction within CON and between CON and other CCRNs, delineating how the interactions changes in different stages of life by dividing the samples into three different age groups and performing analysis in each group. From the perspective of analytical methods, the current study applied a comprehensive analysis based on multiple connection indicators, including classic FC and time-dependent TI and GC, where GC may also provide directional information on the interaction. The approaches applied in the current study help overcome the above-mentioned limitations of the previous study, providing further details of CON-CCRN communication change. The current analysis of the three different age stages clearly demonstrated that CON-CCRN interaction change in a nonmonotonic fashion during the lifetime and the change pattern of each age stage has its own characteristics.

The current study divided the participant into three age groups. The selection of the separating point of the age may affect the result of the connectivity-age joint analysis. The definition of "young", "middle-aged", and "old" may vary in different contexts. The maturing of the brain also showed brain-regional differences and individual differences. Therefore, finding absolute separating points fit-

ting for all conditions is nontrivial and unnecessary. The age of 20 is commonly used to separate mature individuals from immature in daily life, and age 60 is an empirical point that people start recognizing as "old". We tried using the age of 18, 22, 55, or 65, but the results did not change much. Most of the patterns were preserved, indicating that the results were not sensitive to the selection of the empirical separating point.

In this study, we used global signal regression to alleviate the contamination of common noise embedded in the global signal. However, it is worth noting that global signal removal is a common practice in resting-state and task fMRI research, and there are both for and against it. Some people think it may confound the results if the global signal is strongly modulated by the task or other experimental factors [82–84]. Others suggest that it is conducive to observing localized neuronal effects that can be obscured by various global noise factors [85–89]. We proposed whether global signal regression should be performed depending on specific situations, such as different datasets and methodological considerations.

The current study has some limitations. First, it only conducted correlation analysis across participants of different ages. The results may be affected by individual differences across the participants. Because of the limitation of the dataset, each participant accounted for a single time point (the age when scanned), and it is hard to acquire continuous life-long longitudinal MRI data. We could not examine how the CON-CCRN interaction develops and changes within an individual on a life-time level. Second, the current study focused on the linear relationship between connectivity and age; we adopted a classic and intuitive correlation method but could not explore the potential non-linear, complex relationship between connectivity and age. More sophisticated methods for detecting the non-linear trend may be needed in future studies better to delineate potential complex changes in the connection indicators. The current study only focused on the interaction between CON and several well-defined CCRNs. However, it is worth noting that using a data-driven approach across parcels defined by an atlas may provide insightful results that show overall brain connectivity development.

## 5. Conclusions

The study characterizes the changing pattern of the interactions between CON and several well-proposed functional networks (including CON itself, DAN, CEN, and DMN) closely associated with cognitive control at different stages of life. The results indicated the prominently increased integrity of within-CON and CON-CCRN communication, mildly weakened within-CON communication, and significantly attenuated within-CON and CON-DMN communication, characterizing distinct changing patterns of CON-interaction at three different stages that covered a life-long span.

## Availability of Data and Materials

The datasets used and analyzed during the current study are available from the corresponding author on reasonable request.

The datasets generated and analyzed during the current study are available in the Nathan Kline Institute repository, [[http://fcon\\_1000.projects.nitrc.org/indi/pro/nki.html](http://fcon_1000.projects.nitrc.org/indi/pro/nki.html)].

## Author Contributions

XTW designed the study, interpreted the results and wrote the paper; BKH, GDW, FYD, JHZ analyzed the data, interpreted the results, and wrote the paper. All authors contributed to editorial changes in the manuscript. All authors read and approved the final manuscript. All authors have participated sufficiently in the work and agreed to be accountable for all aspects of the work.

## Ethics Approval and Consent to Participate

All participants signed a written informed consent form according to the Helsinki Declaration and satisfied the criteria for MRI. The Ethics Committee of the Department of Psychology at Renmin University of China authorized the current analysis procedure. The ethical approval code provided by the IRB of our institute is 22-068.

## Acknowledgment

Thanks to all the peer reviewers for their opinions and suggestions.

## Funding

The present study was supported by the Fund for Building World-class Universities (disciplines) of Renmin University of China, Major Innovation & Planning Interdisciplinary Platform for the “Double-First Class” Initiative of Renmin University of China.

## Conflict of Interest

The authors declare no conflict of interest.

## References

- [1] Vaden KI, Kuchinsky SE, Cute SL, Ahlstrom JB, Dubno JR, Eckert MA. The cingulo-opercular network provides word-recognition benefit. *The Journal of Neuroscience*. 2013; 33: 18979–18986.
- [2] Haupt M, Ruiz-Rizzo AL, Sorg C, Finke K. Phasic alerting effects on visual processing speed are associated with intrinsic functional connectivity in the cingulo-opercular network. *NeuroImage*. 2019; 196: 216–226.
- [3] Cohen N, Ben-Yakov A, Weber J, Edelson MG, Paz R, Dudai Y. Prestimulus Activity in the Cingulo-Opercular Network Predicts Memory for Naturalistic Episodic Experience. *Cerebral Cortex*. 2020; 30: 1902–1913.
- [4] Seeley WW, Menon V, Schatzberg AF, Keller J, Glover GH, Kenna H, *et al.* Dissociable intrinsic connectivity networks for salience processing and executive control. *The Journal of Neuroscience*. 2007; 27: 2349–2356.
- [5] Penning MD, Ruiz-Rizzo AL, Redel P, Müller HJ, Salminen T, Strobach T, *et al.* Alertness Training Increases Visual Processing Speed in Healthy Older Adults. *Psychological Science*. 2021; 32: 340–353.
- [6] Chen Z, Guo Y, Suo T, Feng T. Coupling and segregation of large-scale brain networks predict individual differences in delay discounting. *Biological Psychology*. 2018; 133: 63–71.
- [7] Peelle JE. Listening Effort: How the Cognitive Consequences of Acoustic Challenge Are Reflected in Brain and Behavior. *Ear and Hearing*. 2018; 39: 204–214.
- [8] Wallis G, Stokes M, Cousijn H, Woolrich M, Nobre AC. Frontoparietal and Cingulo-opercular Networks Play Dissociable Roles in Control of Working Memory. *Journal of Cognitive Neuroscience*. 2015; 27: 2019–2034.
- [9] Dosenbach NUF, Visscher KM, Palmer ED, Miezin FM, Wenger KK, Kang HC, *et al.* A core system for the implementation of task sets. *Neuron*. 2006; 50: 799–812.
- [10] Chai XJ, Castañón AN, Ongür D, Whitfield-Gabrieli S. Anticorrelations in resting state networks without global signal regression. *NeuroImage*. 2012; 59: 1420–1428.
- [11] Goulden N, Khusnulina A, Davis NJ, Bracewell RM, Bokde AL, McNulty JP, *et al.* The salience network is responsible for switching between the default mode network and the central executive network: replication from DCM. *NeuroImage*. 2014; 99: 180–190.
- [12] Shaw SB, McKinnon MC, Heisz J, Becker S. Dynamic task-linked switching between brain networks - A tri-network perspective. *Brain and Cognition*. 2021; 151: 105725.
- [13] Sridharan D, Levitin DJ, Menon V. A critical role for the right fronto-insular cortex in switching between central-executive and default-mode networks. *Proceedings of the National Academy of Sciences of the United States of America*. 2008; 105: 12569–12574.
- [14] Fox MD, Corbetta M, Snyder AZ, Vincent JL, Raichle ME. Spontaneous neuronal activity distinguishes human dorsal and ventral attention systems. *Proceedings of the National Academy of Sciences of the United States of America*. 2006; 103: 10046–10051.
- [15] Curtis CE, D’Esposito M. Persistent activity in the prefrontal cortex during working memory. *Trends in Cognitive Sciences*. 2003; 7: 415–423.
- [16] Ridderinkhof KR, Ullsperger M, Crone EA, Nieuwenhuis S. The role of the medial frontal cortex in cognitive control. *Science*. 2004; 306: 443–447.
- [17] Vatansever D, Menon DK, Stamatakis EA. Default mode contributions to automated information processing. *Proceedings of the National Academy of Sciences of the United States of America*. 2017; 114: 12821–12826.
- [18] Chen AC, Oathes DJ, Chang C, Bradley T, Zhou Z, Williams LM, *et al.* Causal interactions between fronto-parietal central executive and default-mode networks in humans. *Proceedings of the National Academy of Sciences of the United States of America*. 2013; 110: 19944–19949.
- [19] Berman MG, Nee DE, Casement M, Kim HS, Deldin P, Kross E, *et al.* Neural and behavioral effects of interference resolution in depression and rumination. *Cognitive, Affective & Behavioral Neuroscience*. 2011; 11: 85–96.
- [20] Cheng Y, Xue T, Dong F, Hu Y, Zhou M, Li X, *et al.* Abnormal functional connectivity of the salience network in insomnia. *Brain Imaging and Behavior*. 2022; 16: 930–938.
- [21] Uddin LQ, Supekar K, Lynch CJ, Khoutham A, Phillips J, Feinstein C, *et al.* Salience network-based classification and prediction of symptom severity in children with autism. *JAMA Psychiatry*. 2013; 70: 869–879.
- [22] Fair DA, Dosenbach NUF, Church JA, Cohen AL, Brahmbhatt S, Miezin FM, *et al.* Development of distinct control networks

- through segregation and integration. *Proceedings of the National Academy of Sciences of the United States of America*. 2007; 104: 13507–13512.
- [23] Uddin LQ, Supekar KS, Ryali S, Menon V. Dynamic reconfiguration of structural and functional connectivity across core neurocognitive brain networks with development. *The Journal of Neuroscience*. 2011; 31: 18578–18589.
- [24] Marek S, Hwang K, Foran W, Hallquist MN, Luna B. The Contribution of Network Organization and Integration to the Development of Cognitive Control. *PLoS Biology*. 2015; 13: e1002328.
- [25] Baker STE, Lubman DI, Yücel M, Allen NB, Whittle S, Fulcher BD, *et al.* Developmental Changes in Brain Network Hub Connectivity in Late Adolescence. *The Journal of Neuroscience*. 2015; 35: 9078–9087.
- [26] Pozzi E, Vijayakumar N, Byrne ML, Bray KO, Seal M, Richmond S, *et al.* Maternal parenting behavior and functional connectivity development in children: A longitudinal fMRI study. *Developmental Cognitive Neuroscience*. 2021; 48: 100946.
- [27] Yan CG, Wang XD, Zuo XN, Zang YF. DPABI: Data Processing & Analysis for (Resting-State) Brain Imaging. *Neuroinformatics*. 2016; 14: 339–351.
- [28] Friston KJ, Ashburner J, Frith CD, Poline JB, Frackowiak R. Spatial registration and normalization of images. *Human Brain Mapping*. 2010; 3: 165–189.
- [29] Beckmann CF, DeLuca M, Devlin JT, Smith SM. Investigations into resting-state connectivity using independent component analysis. *Philosophical Transactions of the Royal Society of London. Series B, Biological Sciences*. 2005; 360: 1001–1013.
- [30] Glasser MF, Coalson TS, Bijstervosch JD, Harrison SJ, Harms MP, Anticevic A, *et al.* Using temporal ICA to selectively remove global noise while preserving global signal in functional MRI data. *NeuroImage*. 2018; 181: 692–717.
- [31] Power JD, Barnes KA, Snyder AZ, Schlaggar BL, Petersen SE. Spurious but systematic correlations in functional connectivity MRI networks arise from subject motion. *NeuroImage*. 2012; 59: 2142–2154.
- [32] Wen X, Mo J, Ding M. Exploring resting-state functional connectivity with total interdependence. *NeuroImage*. 2012; 60: 1587–1595.
- [33] Wu G, Liao W, Stramaglia S, Ding J, Chen H, Marinazzo D. A blind deconvolution approach to recover effective connectivity brain networks from resting state fMRI data. *Medical Image Analysis*. 2013; 17: 365–374.
- [34] Wu G, Marinazzo D. Sensitivity of the resting-state haemodynamic response function estimation to autonomic nervous system fluctuations. *Philosophical Transactions. Series A, Mathematical, Physical, and Engineering Sciences*. 2016; 374: 20150190.
- [35] Poole VN, Robinson ME, Singleton O, DeGutis J, Milberg WP, McGlinchey RE, *et al.* Intrinsic functional connectivity predicts individual differences in distractibility. *Neuropsychologia*. 2016; 86: 176–182.
- [36] Sadaghiani S, Hesselmann G, Kleinschmidt A. Distributed and antagonistic contributions of ongoing activity fluctuations to auditory stimulus detection. *The Journal of Neuroscience*. 2009; 29: 13410–13417.
- [37] Ptak R. The frontoparietal attention network of the human brain: action, saliency, and a priority map of the environment. *The Neuroscientist*. 2012; 18: 502–515.
- [38] Buckner RL, Andrews-Hanna JR, Schacter DL. The brain's default network: anatomy, function, and relevance to disease. *Annals of the New York Academy of Sciences*. 2008; 1124: 1–38.
- [39] Biswal B, Yetkin FZ, Houghton VM, Hyde JS. Functional connectivity in the motor cortex of resting human brain using echoplanar MRI. *Magnetic Resonance in Medicine*. 1995; 34: 537–541.
- [40] Fox MD, Snyder AZ, Vincent JL, Corbetta M, Van Essen DC, Raichle ME. The human brain is intrinsically organized into dynamic, anticorrelated functional networks. *Proceedings of the National Academy of Sciences of the United States of America*. 2005; 102: 9673–9678.
- [41] Gelfand IM, Yaglom AM. Calculation of the amount of information about a random function contained in another such function. *Mathematical Society Translations, Series*. 1959; 2: 199–246.
- [42] Granger CWJ. Investigating causal relations by econometric models and cross-spectral methods. *Econometrica*. 1969; 37: 424–438.
- [43] Ding M, Bressler SL, Yang W, Liang H. Short-window spectral analysis of cortical event-related potentials by adaptive multivariate autoregressive modeling: data preprocessing, model validation, and variability assessment. *Biological Cybernetics*. 2000; 83: 35–45.
- [44] Ding M, Chen Y, Bressler SL. Granger Causality: Basic Theory and Application to Neuroscience. *Handbook of Time Series Analysis*. 2006; 437–460.
- [45] Wen X, Rangarajan G, Ding M. Multivariate Granger causality: an estimation framework based on factorization of the spectral density matrix. *Philosophical Transactions. Series A, Mathematical, Physical, and Engineering Sciences*. 2013; 371: 20110610.
- [46] Harrison L, Penny WD, Friston K. Multivariate autoregressive modeling of fMRI time series. *NeuroImage*. 2003; 19: 1477–1491.
- [47] Rogers BP, Katwal SB, Morgan VL, Asplund CL, Gore JC. Functional MRI and multivariate autoregressive models. *Magnetic Resonance Imaging*. 2010; 28: 1058–1065.
- [48] Wen X, Liu Y, Zhao P, Liu Z, Li H, Li W, *et al.* Disrupted communication of the temporoparietal junction in patients with major depressive disorder. *Cognitive, Affective & Behavioral Neuroscience*. 2021; 21: 1276–1296.
- [49] Wen X, Li W, Liu Y, Liu Z, Zhao P, Zhu Z, *et al.* Exploring communication between the thalamus and cognitive control-related functional networks in the cerebral cortex. *Cognitive, Affective & Behavioral Neuroscience*. 2021; 21: 656–677.
- [50] Vakamudi K, Posse S, Jung R, Cushnyr B, Chohan MO. Real-time presurgical resting-state fMRI in patients with brain tumors: Quality control and comparison with task-fMRI and intraoperative mapping. *Human Brain Mapping*. 2020; 41: 797–814.
- [51] Wen X, Yao L, Liu Y, Ding M. Causal interactions in attention networks predict behavioral performance. *The Journal of Neuroscience*. 2012; 32: 1284–1292.
- [52] Wen X, Liu Y, Yao L, Ding M. Top-down regulation of default mode activity in spatial visual attention. *The Journal of Neuroscience*. 2013; 33: 6444–6453.
- [53] Zhao P, Yu R, Liu Y, Liu Z, Wu X, Li R, *et al.* The functional hierarchy of the task-positive networks indicates a core control system of top-down regulation in visual attention. *Journal of Integrative Neuroscience*. 2021; 20: 43–53.
- [54] Aben B, Buc Calderon C, Van den Bussche E, Verguts T. Cognitive Effort Modulates Connectivity between Dorsal Anterior Cingulate Cortex and Task-Relevant Cortical Areas. *The Journal of Neuroscience*. 2020; 40: 3838–3848.
- [55] Luna B, Marek S, Larsen B, Tervo-Clemmens B, Chahal R. An integrative model of the maturation of cognitive control. *Annual Review of Neuroscience*. 2015; 38: 151–170.
- [56] Dosenbach NUF, Fair DA, Miezin FM, Cohen AL, Wenger KK, Dosenbach RAT, *et al.* Distinct brain networks for adaptive and stable task control in humans. *Proceedings of the National Academy of Sciences of the United States of America*. 2007; 104: 11073–11078.
- [57] Sbahat H, Rajkumar R, Ramkiran S, Assi AA, Shah NJ, Veselinović T, *et al.* Dynamics of task-induced modulation of

- spontaneous brain activity and functional connectivity in the triple resting-state networks assessed using the visual oddball paradigm. *PLoS ONE*. 2021; 16: e0246709.
- [58] Uddin LQ. Salience processing and insular cortical function and dysfunction. *Nature Reviews. Neuroscience*. 2015; 16: 55–61.
- [59] Touroutoglou A, Hollenbeck M, Dickerson BC, Feldman Barrett L. Dissociable large-scale networks anchored in the right anterior insula subserved affective experience and attention. *NeuroImage*. 2012; 60: 1947–1958.
- [60] Touroutoglou A, Bliss-Moreau E, Zhang J, Mantini D, Vanduffel W, Dickerson BC, *et al.* A ventral salience network in the macaque brain. *NeuroImage*. 2016; 132: 190–197.
- [61] Chong JSX, Ng GJP, Lee SC, Zhou J. Salience network connectivity in the insula is associated with individual differences in interoceptive accuracy. *Brain Structure & Function*. 2017; 222: 1635–1644.
- [62] Fair DA, Cohen AL, Power JD, Dosenbach NUF, Church JA, Miezin FM, *et al.* Functional brain networks develop from a “local to distributed” organization. *PLoS Computational Biology*. 2009; 5: e1000381.
- [63] Soederberg Miller LM, Lachman ME. Cognitive Performance and the Role of Control Beliefs in Midlife. *Aging Neuropsychology and Cognition*. 2000; 7: 69–85.
- [64] Hardin MG, Schroth E, Pine DS, Ernst M. Incentive-related modulation of cognitive control in healthy, anxious, and depressed adolescents: development and psychopathology related differences. *Journal of Child Psychology and Psychiatry, and Allied Disciplines*. 2007; 48: 446–454.
- [65] Yu M, Linn KA, Shinohara RT, Oathes DJ, Cook PA, Duprat R, *et al.* Childhood trauma history is linked to abnormal brain connectivity in major depression. *Proceedings of the National Academy of Sciences of the United States of America*. 2019; 116: 8582–8590.
- [66] Becker H, Norman L, Yang H, Monk C, Phan K, Taylor S, *et al.* Disorder-specific cingulo-opercular network hyperconnectivity in pediatric OCD relative to pediatric anxiety. *Psychological Medicine*. 2021; 1–11.
- [67] Chen J, Shu H, Wang Z, Zhan Y, Liu D, Liao W, *et al.* Convergent and divergent intranetwork and internetwork connectivity patterns in patients with remitted late-life depression and amnesic mild cognitive impairment. *Cortex*. 2016; 83: 194–211.
- [68] Andrews-Hanna JR. The brain’s default network and its adaptive role in internal mentation. *The Neuroscientist*. 2012; 18: 251–270.
- [69] Brewer JA, Worhunsky PD, Gray JR, Tang Y, Weber J, Kober H. Meditation experience is associated with differences in default mode network activity and connectivity. *Proceedings of the National Academy of Sciences of the United States of America*. 2011; 108: 20254–20259.
- [70] Gusnard DA, Raichle ME, Raichle ME. Searching for a baseline: functional imaging and the resting human brain. *Nature Reviews. Neuroscience*. 2001; 2: 685–694.
- [71] Mason MF, Norton MI, Van Horn JD, Wegner DM, Grafton ST, Macrae CN. Wandering minds: the default network and stimulus-independent thought. *Science*. 2007; 315: 393–395.
- [72] Zhang H, Yang S, Qiao Y, Ge Q, Tang Y, Northoff G, *et al.* Default mode network mediates low-frequency fluctuations in brain activity and behavior during sustained attention. *Human Brain Mapping*. 2022; 43: 5478–5489.
- [73] Esposito F, Aragri A, Latorre V, Papolizio T, Scarabino T, Cirillo S, *et al.* Does the default-mode functional connectivity of the brain correlate with working-memory performances? *Archives Italiennes De Biologie*. 2009; 147: 11–20.
- [74] Yuan Y, Pan X, Wang R. Biophysical mechanism of the interaction between default mode network and working memory network. *Cognitive Neurodynamics*. 2021; 15: 1101–1124.
- [75] Melrose RJ, Jimenez AM, Riskin-Jones H, Weissberger G, Veliz J, Hasratian AS, *et al.* Alterations to task positive and task negative networks during executive functioning in Mild Cognitive Impairment. *NeuroImage. Clinical*. 2018; 19: 970–981.
- [76] Mevel K, Chételat G, Eustache F, Desgranges B. The default mode network in healthy aging and Alzheimer’s disease. *International Journal of Alzheimer’s Disease*. 2011; 2011: 535816.
- [77] Barber AD, Jacobson LA, Wexler JL, Nebel MB, Caffo BS, Pekar JJ, *et al.* Connectivity supporting attention in children with attention deficit hyperactivity disorder. *NeuroImage. Clinical*. 2014; 7: 68–81.
- [78] Rektorova I. Resting-state networks in Alzheimer’s disease and Parkinson’s disease. *Neuro-Degenerative Diseases*. 2014; 13: 186–188.
- [79] Godwin D, Ji A, Kandala S, Mamah D. Functional Connectivity of Cognitive Brain Networks in Schizophrenia during a Working Memory Task. *Frontiers in Psychiatry*. 2017; 8: 294.
- [80] Shen X, Cox SR, Adams MJ, Howard DM, Lawrie SM, Ritchie SJ, *et al.* Resting-State Connectivity and Its Association With Cognitive Performance, Educational Attainment, and Household Income in the UK Biobank. *Biological Psychiatry. Cognitive Neuroscience and Neuroimaging*. 2018; 3: 878–886.
- [81] Stephan Y, Sutin AR, Luchetti M, Terracciano A. Subjective age and informant-rated cognition and function: A prospective study. *Psychology and Aging*. 2021; 36: 338–343.
- [82] Aguirre GK, Zarahn E, D’esposito M. The variability of human, BOLD hemodynamic responses. *NeuroImage*. 1998; 8: 360–369.
- [83] Gavrilescu M, Shaw ME, Stuart GW, Eckersley P, Svalbe ID, Egan GF. Simulation of the effects of global normalization procedures in functional MRI. *NeuroImage*. 2002; 17: 532–542.
- [84] Junghöfer M, Schupp HT, Stark R, Vaitl D. Neuroimaging of emotion: empirical effects of proportional global signal scaling in fMRI data analysis. *NeuroImage*. 2005; 25: 520–526.
- [85] Birn RM, Diamond JB, Smith MA, Bandettini PA. Separating respiratory-variation-related fluctuations from neuronal-activity-related fluctuations in fMRI. *NeuroImage*. 2006; 31: 1536–1548.
- [86] Fox MD, Zhang D, Snyder AZ, Raichle ME. The global signal and observed anticorrelated resting state brain networks. *Journal of Neurophysiology*. 2009; 101: 3270–3283.
- [87] Glover GH, Li TQ, Ress D. Image-based method for retrospective correction of physiological motion effects in fMRI: RETROICOR. *Magnetic Resonance in Medicine*. 2000; 44: 162–167.
- [88] Lund TE, Madsen KH, Sidaros K, Luo W, Nichols TE. Non-white noise in fMRI: does modelling have an impact? *NeuroImage*. 2006; 29: 54–66.
- [89] Wise RG, Ide K, Poulin MJ, Tracey I. Resting fluctuations in arterial carbon dioxide induce significant low frequency variations in BOLD signal. *NeuroImage*. 2004; 21: 1652–1664.